

POWER ALLOCATION DESIGN USING GAME THEORY FOR FAST-FADING NON-ORTHOGONAL MEDIUM ACCESS NETWORK

Vishalakshi, Gangadhar Shivsharanappa Biradar*

Department of Electronics and Communication Engineering, PDA College of Engineering, Affiliated to Visvesvaraya Technological University-590018, Belagavi, Kalaburagi, Karnataka, India

* Corresponding Author, e-mail: researchvishalakshi@gmail.com

Abstract: This work addresses critical challenge of efficient Power Allocation (PA) in Multi-Carrier Non-Orthogonal Multiple Access (MC-NOMA) systems for 5G/6G wireless networks under dynamic channel conditions. A novel Game Theory-based Aware Power Allocation Optimization (GTA-PAO) model is proposed to optimize the sum-rate while reducing energy consumption. The methodology integrates mobility effects, imperfect Channel State Information (CSI), and Peak-to-Average Power Ratio (PAPR) reduction to ensure robustness in fast-fading environments. Simulation results in highway and expressway scenarios demonstrate significant performance gains, including notable reductions in Bit Error Rate (BER) and PAPR alongside considerable improvements in sum-rate. The findings confirm that the GTA-PAO framework enhances adaptability and efficiency, making it a strong candidate for practical deployment in next-generation wireless communication systems.

Key words: MC-NOMA, power allocation, game theory, sum-rate, 5G, CSI, mobility.

1. INTRODUCTION

Non-Orthogonal Multiple Access (NOMA) has emerged as a pivotal technology for 5G and the upcoming 6G wireless communication systems. Unlike traditional orthogonal multiple access (OMA) schemes that assign exclusive time-frequency resources to users, NOMA allows multiple users to simultaneously share the same resource block through power domain multiplexing [1]. Traditional OMA systems suffer from inter-user interference, which can degrade system performance. NOMA, on the other hand, embraces this interference model by using superposition coding and Successive Interference Cancellation (SIC) [2]. The integration of Multiple Input Multiple Output (MIMO) technology with NOMA (i.e., MIMO-NOMA) further amplifies these benefits. However, in Multi-Carrier NOMA (MC-NOMA) systems, Power Allocation (PA) becomes a critical challenge. Hence, efficient PA is necessary to

ensure fair signal distribution among users and to preserve the performance benefits of NOMA. Also, the PA strategy must consider factors such as channel conditions, interference levels, and varying user demands.

Further, Channel State Information (CSI) is essential in optimizing PA and resource allocation in NOMA systems. CSI provides vital insights into the communication link between users and the base station (BS), guiding power control decisions. Nevertheless, assuming perfect CSI is unrealistic due to inherent channel estimation errors and the limitations of SIC in practical implementations [3]. Many existing studies simplify system design by presuming perfect CSI [4, 5], overlooking the impact of inaccuracies and fairness concerns [6]. Fairness in resource allocation remains a major issue when CSI is imperfect, potentially resulting in uneven service quality across users. In addition, NOMA faces several challenges, including user mobility, high peak-to-average power ratio (PAPR), and the effects of fast-fading multipath propagation. These practical considerations must be addressed for reliable and scalable NOMA deployment. Several existing solutions, particularly those employing Reinforcement Learning and Game Theory (GT), have been proposed to resolve the PA problem in NOMA networks [7]-[9]. GT provides a robust mathematical approach for modeling user interactions and optimizing PA strategies in dynamic environments. Motivated by these challenges, this work proposes a Game Theory-based Power Allocation Optimization (GTA-PAO) framework designed specifically for large-scale MC-NOMA networks. The main contributions of this paper are summarized as follows.

- A novel PA scheme is designed for Multi-Carrier NOMA systems.
- A GT model is developed to enhance system sum-rate while minimizing power consumption, thereby meeting PAPR constraints.
- A new utility function optimization method is proposed, which leverages user cooperation to improve performance in MC-NOMA.
- The proposed model, called Game-Theory Aware Power Allocation Optimization (GTA-PAO), is robust against diverse fast-fading conditions, including highway and expressway mobility scenarios.
- GTA-PAO demonstrates significant reductions in both PAPR and Bit Error Rate (BER) compared to state-of-the-art techniques.
- The GTA-PAO achieves superior sum-rate performance under various deployment conditions.

The manuscript organization is as follows. Section II discusses the current working of the PA design for NOMA and its limitations. Section III discusses the working of the GTA-PAO design for MC-NOMA. Section IV discusses the results achieved using GTA-PAO over the existing PA design. Section V discusses research significance and its future enhancement.

2. LITERATURE SURVEY

The literature survey discusses the current working of PA design for NOMA and its limitations. In [10], focus was on optimizing decoding order and PA in two-user uplink Cooperative NOMA (C-NOMA), where aimed at to maximize the minimum achievable data-rate across users. Simulation results showed that by prioritizing decoding of distant

users at the BS enhance overall system throughput, showing the effectiveness of user cooperation in uplink C-NOMA. In [11], addressed dynamic user-allocation in MEC (Mobile Edge-Computing) systems integrated with NOMA, for reducing both PA delay costs and transmission power; hence, modelled stochastic multi-cell, multi-channel environment was modeled where user departures and arrivals impacted resource availability. A distributed Game-Theory (GT) approach was presented for managing PA and the user-channel efficiently. Experimental evaluations on simulated MEC environments showed that the approach outperformed existing approaches, showing better energy efficiency and effective trade-offs among communication resources.

In [12] introduced an optimization strategy using the Coherent-Ising Machine (CIM) was introduced to address channel allocation in NOMA systems, where resource distribution poses an NP-hard challenge. Simulations were carried out to evaluate performance across multiple scenarios, including variations in user count, transmission rates, and available channels, where the CIM approach significantly improved sum-throughput, demonstrating its potential for scalable and high-performance NOMA resource optimization. In [13] proposed a hybrid NOMA-TDMA approach was proposed aimed at maximizing sum-throughput in Internet of Things (IoT) networks. The approach enabled downlink communication using hybrid access points and supported uplink transmission through energy harvesting at user devices. Simulation-based evaluation demonstrated improvements in both throughput and time-slot efficiency, highlighting the hybrid scheme's suitability for energy-constrained IoT environments.

In [14], presented SAFE-GF-NOMA architecture was presented, which enhanced spatial capacity through autonomous social interactions among IoT devices. The system leveraged grant-free NOMA for uplink communication while mitigating collision issues through a Social IoT (SIoT) framework. Simulation results showed a 50% reduction in collision probability, over 50% increase in successful transmissions, and a threefold improvement in network capacity. Energy consumption was also significantly reduced, from 17 J to 5 J per device. In [15], an advanced decoding approach for uplink NOMA systems was presented, introducing the Successive-Parzen-Windows Interference Cancellation (SPWIC) technique. Utilizing 3D antenna configurations, SPWIC applied a non-parametric density estimation method to better distinguish and decode overlapping signals. Performance assessments demonstrated that SPWIC outperformed traditional SIC methods in terms of decoding accuracy and signal separation, particularly under high user density and spatial complexity.

In [16], a resource optimization framework for MIMO-NOMA systems was proposed, incorporating multi-path routing and dynamic link scheduling for improving transmission power distribution. The method demonstrated enhancements in latency, sum-throughput, sum-rate, and fairness. Similarly, [17] introduced a hybrid multiple access scheme using Intelligent Reflecting Surfaces (IRS) to boost system throughput. Results showed significant improvements in phase configuration, scheduling efficiency, and overall network throughput compared to conventional systems. In [18], growing demands of IoT networks were addressed by introducing Throughput-Enhanced Resource-Management (TERM), where the objective was to improve the sum throughput and reduce outage probability in environments affected by interference and

path loss. TERM employed an XGBoost-based model for predictive resource allocation and adaptive power control. Simulation results highlight its effectiveness, showing a 23.37% increase in average sum throughput, 31.34% decrease in outage probability, and 87.55% reduction in BER, outperforming conventional resource management methods.

Existing PA techniques for NOMA networks, while innovative, exhibit notable limitations in practical deployments, like, in [10] addressed PA and decoding in cooperative uplink NOMA but restricted their model to two users, limiting scalability. In [11] employed Lyapunov and GT methods were employed in MEC-integrated NOMA systems, but did not fully address fast-fading or fairness under complex dynamics. Similarly, in [12] used CIM was used for optimal channel assignment, but the high computational complexity limits real-time applicability. Hybrid schemes like the NOMA-TDMA model [13] and SAFE-GF-NOMA [14] focused on energy efficiency and access fairness but lacked comprehensive PA models under high mobility or fading conditions. To address these challenges, the proposed GTA-PAO approach introduces a scalable, multi-user PA scheme designed for MC-NOMA. It incorporates a novel utility function considering user cooperation and dynamic channel conditions, effectively handling mobility, PAPR, and BER. Unlike prior models, GTA-PAO ensures optimal power distribution, maintaining system fairness and enhancing sum-rate even in high-density, fast-fading environments, making it more robust for next-generation NOMA applications. In the next section, the GTA-PAO approach is discussed in detail.

3. METHODOLOGY

This work examines a downlink MC-NOMA system, where the BS overlays information intended for M users within a single subcarrier. This is in contrast to the MC-OMA system, in which each user's information is transmitted over a distinct subcarrier. The MC-NOMA signal transmitted from the BS is represented as y_o using Eq. (1).

$$y_o = \frac{1}{\sqrt{O}} \sum_{l=1}^L (\sum_{n=1}^N \sqrt{\beta_{l,n} Q_l B_{l,n}}) e^{-k \frac{2n}{O}} \quad 0 \leq o \leq N - 1 \quad (1)$$

In Eq. (1), O indicates the total number of domain samples in the MC symbol, L indicates the total number of subcarriers within the MC symbol, N represents the number of superposed users on each subcarrier, $\beta_{l,n}$ denotes the PA ratio for n^{th} user on l^{th} subcarrier, Q_l is power allocated to l^{th} subcarrier, $B_{l,n}$ denotes information intended for n^{th} user on l^{th} subcarrier and e^{-k} denotes a constant. Moreover, Eq. (1) represents the total number of time-domain samples in the MC-NOMA symbol, which is equal to the number of data subcarriers, i.e., $O = L$, under the condition that the Nyquist rate matches the sampling frequency. However, when the signal is oversampled by a factor M , the total number of time-domain samples becomes $M \times L$. This oversampled signal is obtained by inserting $(M - 1)L$ zeros into the center of the input frequency-domain vector B , before applying IFFT. The PA ratio, denoted as $\beta_{l,n}$ in Eq. (1) is inversely proportional to the channel condition of each user in a fast-fading environment. When users are sorted based on their channel gains from strongest (near) to weakest (far), the PA coefficients follow the order as presented in Eq. (2).

$$\beta_{l,1} < \dots < \beta_{l,n} < \dots < \beta_{l,n} \text{ Subject } \sum_{n=1}^N \beta_{l,n} \quad (2)$$

For mitigating edge interference, a small number of subcarriers at the boundaries of the MC-NOMA symbol are intentionally set to zero. These subcarriers do not carry user information and act as guard bands. Let L_E denote the number of active data subcarriers. Consequently, the number of null subcarriers is $L - L_E$, with half of them positioned at each edge. These $\frac{L-L_E}{2}$ subcarriers on either side serve as guard bands to suppress Inter-Symbol Interference (ISI). The input vector B_l for Inverse-Fast Fourier-Transform (IFFT) is constructed using the process presented in Eq. (3).

$$B_l = \sum_{n=1}^N B_{l,n} \tag{3}$$

The resulting signal for l^{th} data subcarrier, intended for n^{th} user is denoted as $Z_{l,n}$ using Eq. (4).

$$Z_{l,n} = I_{l,n} \left(\sum_{n=1}^N \sqrt{\beta_{l,n} Q_l B_{l,n}} \right) + O_{l,n} \quad \frac{1 \leq l \leq L}{1 \leq n \leq N} \tag{4}$$

In Eq. (4), $I_{l,n}$ denotes channel-frequency response between n^{th} user and BS at the corresponding subcarrier, $O_{l,n}$ denotes Additive White Gaussian Noise (AWGN) at n^{th} user on l^{th} data subcarrier in the frequency domain, characterized by zero-mean and variance σ_n^α . In Eq. (4), the $I_{l,n}$ is evaluated using Eq. (5).

$$I_{l,n} = \frac{h_{l,n}}{\sqrt{1+d_n^\alpha}} \tag{5}$$

In Eq. (5), $h_{l,n}$ denotes the fast-fading channel coefficient between n^{th} user and BS on l^{th} data subcarrier. Moreover, SIC was employed at the receiver for isolating and removing interference from other superposed users, thereby providing accurate extraction of each user's signal. This is achieved by subtracting signals decoded by weaker users (i.e., user's j where $j > n$) from the signal received at n^{th} user's terminal. In contrast, signals of stronger users (i.e., user's j where $j < n$) are treated as interference in this work. Accordingly, the achievable normalized sum-rate for n^{th} user is computed using Eq. (6).

$$S_n = \sum_{l=1}^L \log_2(1 + \delta_{l,n}) \tag{6}$$

In Eq. (6), S_n denotes the normalized data rate for n^{th} user and $\delta_{l,n}$ represents Signal-to-Noise Ratio (SNR) and Signal-to-Interference-Noise Ratio (SINR), for n^{th} user on l^{th} subcarrier. The $\delta_{l,n}$ is evaluated using Eq. (7).

$$\delta_{l,n} = \frac{Q_l |I_{l,n}|^2 \beta_{l,n}}{(Q_l |I_{l,n}|^2 \sum_{j=1}^{n-1} \beta_{l,n}) + \sigma_{l,n}^2} = \frac{\tau_l |I_{l,n}|^2 \beta_{l,n}}{(\tau_l |I_{l,n}|^2 \sum_{j=1}^{n-1} \beta_{l,n}) + 1} \tag{7}$$

In Eq. (7), $\frac{Q_l}{\sigma_{l,n}^2} \cong \tau_{l,n}$, i.e., the first term in the denominator in Eq. (7) becomes zero when evaluating $\delta_{l,1}$ as this user is assumed to be closest to BS and thus experiences negligible interference. Using the following condition, the total sum-rate presented in Eq. (6) is computed using Eq. (8), followed by Eq. (9).

$$S_{l,n} = \sum_{n=1}^N S_n = \sum_{n=1}^N \log_2 \prod_{l=1}^L \left(1 + C \frac{\tau_l |I_{l,n}|^2 \beta_{l,n}}{(\tau_l |I_{l,n}|^2 \sum_{j=1}^{n-1} \beta_{l,n}) + 1} \right) \tag{8}$$

$$S_{TOTAL} = \sum_l \sum_{n=1}^{n/2-1} S_{l,n} \tag{9}$$

In Eq. (8), C is an optimization constant. However, using Eq. (9) may lead to higher PAPR, along with reduced power efficiency and lower overall sum-rate. To address these limitations and enhance the system performance of the total sum-rate, this work

introduces the GT model, which aims to maximize sum-rate while minimizing power consumption under various fast-fading interference scenarios. Moreover, the proposed GT model is designed by incorporating two key aspects: the relationship between BS and users and cooperation among users themselves. Furthermore, the utility function for players in the GT model is defined using Eq. (10) and Eq. (11).

$$U_1^o = \varphi * S_1^o + \omega * C_3^\tau - \mu * C_3^\tau \quad (10)$$

$$U_2^o = \varphi * S_2^o + \omega * C_3^\rho - \mu * C_3^\rho \quad (11)$$

In Eq. (10) and Eq. (11), ω and φ denote constants denoting subscription charges for PA and sum-rate S_1^o and S_2^o respectively. The PA from BS-1 to BS-2 is denoted using C_3^τ and C_3^ρ , while μ denotes the objective cost function associated with resource utilization. The objective cost function adopted in this work is similar to that presented in [12]. From this the μ is evaluated using Eq. (12).

$$\mu = y + z(C_3^\tau + C_3^\rho)^\alpha \quad (12)$$

In Eq. (12), α , y and z are non-negative constant variables, where $\alpha \geq 1$ ensures the convexity of the objective cost function. Eq. (12) also presents the overall cost incurred by BS, which increases PA to every cooperative terminal. To address this, consider BS denoted as B_2 , which seeks to maximize the utility function by individually increasing PA for every user. Through this approach, the total cost for all BSs can be optimized more effectively. However, increasing PA at B_2 results decrease in the utility function of BS B_1 , thereby allowing B_1 to retain more power for resource allocation and PA compared to B_2 . This scenario reflects a fundamental trade-off between power consumption and achievable sum-rate, which is evaluated using Eq. (13).

$$q_3 \propto \frac{1}{C_3^\tau + C_3^\rho} \quad (13)$$

The Eq. (13) can be further simplified into Eq. (14) and Eq. (15).

$$[O_0 + H_{3B_1} q_3] = \frac{a_1}{C_3^\tau} \quad (14)$$

$$[O_0 + H_{3B_2} q_3] = \frac{a_2}{C_3^\rho} \quad (15)$$

In Eq. (14) and Eq. (15), a_1 and a_2 are non-negative constant variables. Based on this simplification, Eq. (10) and Eq. (11) are reformulated as presented in Eq. (16) and Eq. (17).

$$V_1^o = \varphi * S_1^o + \omega * C_3^\tau - \left[y + z(C_3^\tau + C_3^\rho)^\alpha \right] * C_3^\tau \quad (16)$$

$$V_2^o = \varphi * S_2^o + \omega * C_3^\rho - \left[y + z(C_3^\tau + C_3^\rho)^\alpha \right] * C_3^\rho \quad (17)$$

Finally using Eq. (16) and Eq. (17), the optimal strategy for efficient PA at the cooperative terminal is expressed using Eq. (18), such that $C_\downarrow \leq C_3^\tau + C_3^\rho \leq C_\uparrow$, $0 \leq C_3^\tau \leq C_1$, $0 \leq C_3^\rho \leq C_2$, $\varphi, \omega, y, z > 0$, $a_1, a_2 \geq 0$, $\alpha \geq 1$.

$$\max V_n^o(C_3^\tau + C_3^\rho) \quad (18)$$

In Eq. (18), C_\downarrow and C_\uparrow are the minimum and maximum bandwidth requirements for cooperating pairing. A key aspect of this work is use of C_\downarrow for regulating cooperative transmission power, thereby reducing interference between BS and mobile terminals. Since a cooperative channel facilitates resource sharing between two cells, the resources allocated to the cooperative terminal by BSs must not exceed the PA limits for mobile

terminals in each respective cell. As a result, the following constraint has to be satisfied as presented in Eq. (19)

$$0 \leq C_3^\tau \leq C_1 \text{ and } 0 \leq C_3^\rho \leq C_2 \tag{19}$$

For determining effective PA, the Nash Equilibrium (NE) is employed by identifying an optimal strategy function for each player, as presented in Eq. (20), such that $C_\downarrow \leq C_3^\tau + C_3^\rho \leq C_\uparrow, 0 \leq C_3^\tau \leq C_1, 0 \leq C_3^\rho \leq C_2, \varphi, \omega, \gamma, z > 0, a_1, a_2 \geq 0, \alpha \geq 1$.

$$(\hat{C}_3^\tau, \hat{C}_3^\rho) = \text{arg max } V_n^o(C_3^\tau, C_3^\rho) \tag{20}$$

Furthermore, to achieve NE for the fixed-game model defined in Eq. (16) and Eq. (17), the utility function V_n^o is differentiated with respect to C_3^τ and C_3^ρ , leading to Eq. (21).

$$GT = \begin{cases} \frac{\partial V_1^o(C_3^\tau, C_3^\rho)}{\partial V_3^\tau} = 0 \\ \frac{\partial V_2^o(C_3^\tau, C_3^\rho)}{\partial V_3^\rho} = 0 \\ 0 \leq C_3^\tau \leq C_1 \\ 0 \leq C_3^\rho \leq C_1 \\ C_\downarrow \leq C_3^\tau \leq C_3^\rho \leq C_\uparrow \end{cases} \tag{21}$$

Using the GT in Eq. (21), the proposed GTA-PAO demonstrates improved performance, as discussed in detail in the experimental results section.

4. RESULTS AND DISCUSSION

This study evaluates the performance of the GTA-PAO model in comparison with three benchmark models: Optimal T and w_0 [13], Proposed [17], and TERM [18]. All models were implemented using the NYUSIM channel simulator [19] (version 2.0) within a MATLAB R2018a framework. To simulate a fast-fading environment and incorporate node mobility, SIMITS [20] and C# programming were utilized, respectively, through MATLAB's .NET integration interface. The comprehensive simulation parameters and configurations were as follows: the carrier frequency was set to 28 GHz with a system bandwidth of 100 MHz and a subcarrier spacing of 15 kHz. The transmit power of each BS was configured to 30 dBm, while each vehicle node transmitted at 23 dBm. A uniform linear antenna array (ULA) with 8 elements was employed at the BS and two elements at the vehicular node, with hybrid beamforming used for directional transmission. The NYUSIM channel model was configured with its default Urban Microcell (UMi) and Rural Macrocell (RMA) parameters, adapted for expressway and highway environments, respectively. The vehicle speeds varied between 60 km/h and 120 km/h for expressway simulations and 100 km/h to 180 km/h for highway scenarios. Node density ranged from 20 to 60 vehicles/km, and mobility was modeled using the Gauss–Markov model implemented using SIMITS. The modulation scheme was 16-QAM, with 64 subcarriers and a cyclic prefix ratio of 1/8. The SNR values ranged from -4 dB to 4 dB. Each experiment was executed over 100 Monte Carlo iterations to ensure statistical reliability, and the simulation duration was set to 10 seconds per run. These configurations ensure the reproducibility of the simulation results.

Figures 1 and 2 illustrate the sum-rate performance of various schemes under varying SNR conditions for expressway and highway environments, respectively. Across both scenarios, the proposed GTA-PAO model consistently outperforms the reference methods, i.e., Optimal T and w_0 , Proposed Scheme, and TERM, demonstrating superior throughput efficiency. In the expressway scenario (Figure 1), the GTA-PAO model delivers the highest sum-rate values at all SNR levels. At 0 dB, it achieves a sum rate of 16.53 Mbps, compared to 10.45 Mbps, 11.45 Mbps, and 14.11 Mbps for Optimal T and w_0 , Proposed Scheme, and TERM, respectively. The relative performance gain of GTA-PAO over Optimal T and w_0 ranges from 32% to 37%, while improvements over the Proposed Scheme and TERM remain significant, averaging 30% and 12%, respectively. Although TERM narrows the gap at higher SNRs (e.g., only ~7.5% difference at 4 dB), GTA-PAO maintains its lead across all conditions.

In the highway scenario (Figure 2), a similar trend is observed. GTA-PAO achieves 19.36 Mbps at 4 dB, outperforming Optimal T and w_0 (11.78 Mbps), Proposed Scheme (12.78 Mbps), and TERM (17.82 Mbps). The performance gap remains substantial, with GTA-PAO showing an average improvement of over 38% relative to Optimal T and w_0 , and over 33% against the Proposed Scheme across the SNR range. While TERM again approaches GTA-PAO performance at higher SNRs, particularly at 2 dB and 4 dB, the GTA-PAO model still maintains an edge in throughput and consistency. These results confirm the effectiveness of GTA-PAO in achieving higher sum rates in both expressway and highway environments. The improvement is particularly notable at lower SNR levels, which are more susceptible to fast-fading and mobility-related disruptions, highlighting GTA-PAO’s robustness in realistic V2X channel conditions.

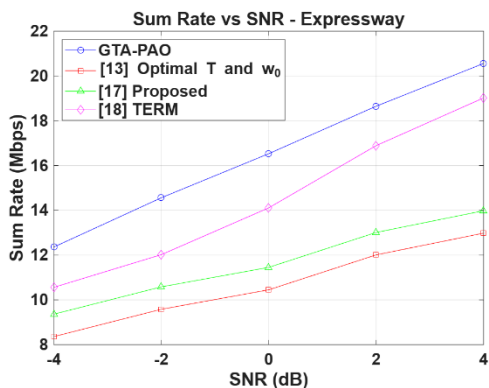


Figure 1. Sum-rate performance under varied SNR for the expressway scenario

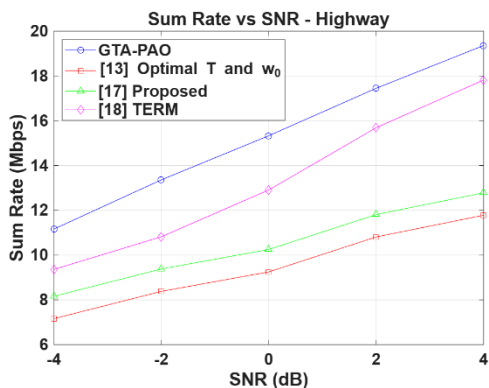


Figure 2. Sum-rate performance under varied SNR for the highway scenario.

Figures 3 and 4 illustrate the BER performance of different models under varying SNR conditions for expressway and highway scenarios, respectively. In both environments, the proposed GTA-PAO model consistently outperforms existing models, Optimal T and w_0 , Proposed Scheme, and TERM, across all SNR values. For the expressway scenario (Figure 3), GTA-PAO achieves significantly lower BER values compared to the other schemes. At an SNR of 0 dB, GTA-PAO records a BER of

0.001658, while Optimal T and w_0 , Proposed Scheme, and TERM report higher BERs of 0.01421, 0.01766, and 0.001871, respectively. The relative improvement of GTA-PAO over Optimal T and w_0 reaches up to 91.96% at 2 dB, while improvement over the Proposed Scheme peaks at 93.65%. When compared to TERM, GTA-PAO also shows meaningful gains, although the margin is smaller, ranging from 5.81% to 11.38%, indicating TERM's relatively stronger performance among existing models.

In the highway scenario (Figure 4), the superiority of GTA-PAO becomes even more pronounced. The BER reduction is most significant at 0 dB, where GTA-PAO achieves 0.0001071, whereas the other schemes register BERs between 0.001871 and 0.008871. The GTA-PAO model demonstrates average improvements of 98.02%, 98.79%, and 94.28% over Optimal T and w_0 , Proposed Scheme, and TERM, respectively, at 0 dB. At higher SNR values (4 dB), GTA-PAO nearly eliminates bit errors, showing a BER of just 9.29×10^{-6} , while the competing models still exhibit BERs in the range of 10^{-3} to 10^{-4} . The results clearly demonstrate the robustness and effectiveness of the GTA-PAO model in fast-fading environments typical of both expressway and highway conditions. Its ability to maintain low BERs across a wide SNR range suggests its strong potential for deployment in high-mobility vehicular communication systems.

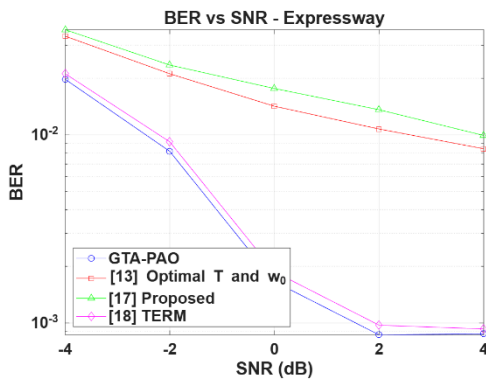


Figure 3. BER performance under varied SNR for the expressway scenario.

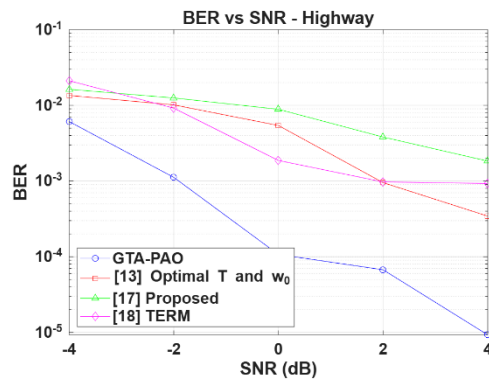


Figure 4. BER performance under varied SNR for the highway scenario.

Figures 5 and 6 analyze the PAPR performance of different schemes under varying SNR conditions in expressway and highway scenarios, respectively. The proposed GTA-PAO model demonstrates notably better PAPR reduction capabilities compared to existing models, Optimal T and w_0 , Proposed Scheme, and TERM. In the expressway scenario (Figure 5), GTA-PAO achieves the lowest PAPR values across all SNR levels. For instance, at an SNR of 0 dB, GTA-PAO records a PAPR of 0.000978, while the other schemes report significantly higher values—0.000991 for Optimal T and w_0 , 0.004371 for Proposed Scheme, and 0.000971 for TERM. On average, GTA-PAO shows an improvement of up to 99.42% over the Proposed Scheme and over 75% improvement compared to Optimal T and w_0 at lower SNR levels. Although TERM exhibits relatively competitive performance at certain points, particularly at 0 dB and 2 dB, the overall

consistency and lower average PAPR achieved by GTA-PAO make it the superior method.

In the highway scenario (Figure 6), the performance advantage of GTA-PAO becomes even more evident, especially at moderate-to-high SNR values. At 0 dB, GTA-PAO reports a remarkably low PAPR of 0.0001071, as opposed to 0.00099102, 0.00437102, and 0.00097102 for Optimal T and w_0 , Proposed Scheme, and TERM, respectively. The average improvement of GTA-PAO over the Proposed Scheme is as high as 97.55%–99.38% across all SNR levels. While TERM occasionally records slightly lower PAPR (e.g., at 2 dB), it also shows negative relative gains, suggesting less stability and higher fluctuation in its performance under highway conditions. These results reinforce the efficiency and robustness of the GTA-PAO model in reducing PAPR, a critical parameter for ensuring power-efficient and distortion-free signal transmission, especially in fast-fading and high-mobility vehicular networks. Its consistently superior performance across both scenarios underscores its practical applicability in real-world 5G and beyond V2X communications.

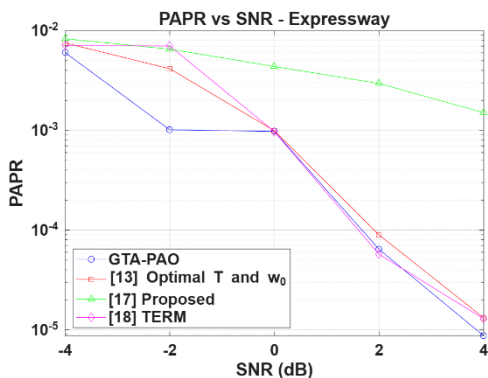


Figure 5. PAPR performance under varied SNR for the expressway scenario.

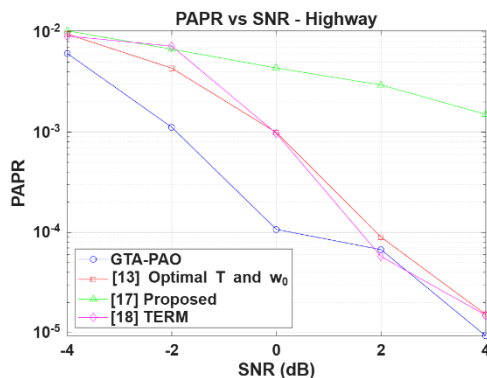


Figure 6. PAPR performance under varied SNR for the highway scenario.

5. CONCLUSION

This study has proposed a downlink MC-NOMA system enhanced by the GTA-PAO model and benchmarked its performance against a conventional MC-OMA system. In the proposed framework, the base station overlays multiple users' signals on the same subcarrier, while a Guarding-Band strategy mitigates inter-channel interference by assigning null subcarriers at spectrum edges. The GTA-PAO model employs IFFT-based processing and dynamically adjusts power allocation based on individual user channel conditions in fast-fading environments. Each user's SINR is evaluated, and SIC is applied at the receiver to recover data accurately. Additionally, a GT model is incorporated to optimize sum-rate, power distribution, and cost, balancing throughput maximization with energy efficiency. Simulation results demonstrate that GTA-PAO consistently outperforms existing schemes in terms of sum-rate, BER, and PAPR across both expressway and highway scenarios, highlighting its robustness under high-mobility and fast-fading conditions. These findings confirm GTA-PAO as a promising solution

for next-generation downlink wireless communications. Future research may focus on integrating adaptive network selection mechanisms to further enhance mobility management, spectral efficiency, and overall network performance.

REFERENCES

- [1] Mohsan, S.A.H., Sadiq, M., Li, Y., Shvetsov, A.V., Shvetsova, S.V., Shafiq, M. NOMA-Based VLC Systems: A Comprehensive Review. *Sensors*, vol.23, no.6, 2023, p.2960. DOI: 10.3390/s23062960.
- [2] Bisen, S., Bhatia, V., Brida, P. Successive interference cancellation with multiple feedback in NOMA-enabled massive IoT network. *EURASIP Journal on Wireless Communications and Networking*, vol.2024, no.1, 2024. DOI: 10.1186/s13638-024-02404-1.
- [3] Liesegang, S., Pascual-Iserte, A., Muñoz, O. Robust design of reconfigurable intelligent surfaces for parameter estimation in MTC. *EURASIP Journal on Wireless Communications and Networking*, vol.2025, no.1, 2025. DOI: 10.1186/s13638-025-02445-0.
- [4] Zhou, W., Xia, J., Li, C., Fan, L., Nallanathan, A. Joint Precoder, Reflection Coefficients, and Equalizer Design for IRS-Assisted MIMO Systems. *IEEE Transactions on Communications*, vol.70, no.6, 2022, pp.4146–4161. DOI: 10.1109/TCOMM.2022.3168284.
- [5] Gao, W., et al. Robust Energy-Efficient Transmission for Cell-Free Massive MIMO Systems with Imperfect CSI. *Electronics*, vol.12, no.16, 2023, p.3384. DOI: 10.3390/electronics12163384.
- [6] Magbool, A., Kumar, V., Flanagan, M.F. Robust Beamforming Design for Fairness-Aware Energy Efficiency Maximization in RIS-Assisted mmWave Communications. *IEEE Transactions on Communications*, vol.73, no.4, 2025, pp.2648–2662. DOI: 10.1109/TCOMM.2024.3466918.
- [7] Wu, Q., et al. Deep Reinforcement Learning-Based Power Allocation for Minimizing Age of Information and Energy Consumption in Multi-Input Multi-Output and Non-Orthogonal Multiple Access Internet of Things Systems. *Sensors*, vol.23, no.24, 2023, p.9687. DOI: 10.3390/s23249687.
- [8] Sun, M., Zhong, Y., He, X., Zhang, J. Channel and Power Allocation for Multi-Cell NOMA Using Multi-Agent Deep Reinforcement Learning and Unsupervised Learning. *Sensors*, vol.25, no.9, 2025, p.2733. DOI: 10.3390/s25092733.
- [9] Gupta, R., Gupta, J. Future generation communications with game strategies: A comprehensive survey. *Computer Communications*, vol.192, 2022, pp.1–32. DOI: 10.1016/j.comcom.2022.05.024.
- [10] Elhattab, M., Arfaoui, M.A., Assi, C., Ghrayeb, A., Qaraqe, M. Power Allocation Optimization and Decoding Order Selection in Uplink C-NOMA Networks. *IEEE Communications Letters*, vol.27, no.1, 2023, pp.352–356. DOI: 10.1109/LCOMM.2022.3214445.
- [11] Lai, P., et al. Online User and Power Allocation in Dynamic NOMA-Based Mobile Edge Computing. *IEEE Transactions on Mobile Computing*, vol.22, no.11, 2023, pp.6676–6689. DOI: 10.1109/TMC.2022.3193366.
- [12] Otsuka, T., Li, A., Takesue, H., Inaba, K., Aihara, K., Hasegawa, M. High-Speed Resource Allocation Algorithm Using a Coherent Ising Machine for NOMA Systems. *IEEE*

- Transactions on Vehicular Technology*, vol.73, no.1, 2024, pp.707–723. DOI: 10.1109/TVT.2023.3300920.
- [13] Afridi, A., Hameed, I., García, C.E., Koo, I. Throughput Maximization of Wireless Powered IoT Network with Hybrid NOMA-TDMA Scheme: A Genetic Algorithm Approach. *IEEE Access*, vol.12, 2024, pp.65241–65253. DOI: 10.1109/ACCESS.2024.3396497.
- [14] Kumbhar, F.H., Unar, S., Mesbah, W., Benevides da Costa, D. SAFE-GF-NOMA: Social Autonomous Flocking to Enhance GF-NOMA for Massive Internet of Things Uplink Access Contention. *IEEE Access*, vol.12, 2024, pp.96085–96099. DOI: 10.1109/ACCESS.2024.3427013.
- [15] Jiménez, V.P.G., Vázquez, Á.N. Uplink Non-Orthogonal Multiple Access (NOMA) Decoding Based on Successive Parzen Windows Interference Cancellation. *IEEE Open Journal of Vehicular Technology*, vol.6, 2025, pp.265–275. DOI: 10.1109/OJVT.2024.3513460.
- [16] Cho, C.-W., Pan, M.-S. Resource Scheduling in MU-MIMO and NOMA-Enabled Integrated Access and Backhaul Networks. *IEEE Open Journal of the Communications Society*, 2025. DOI: 10.1109/OJCOMS.2025.3525506.
- [17] Ma, Y., Wu, R., Zhang, Y., Shang, Y., Zhu, L. Throughput Maximization for IRS-Assisted WPCN With Hybrid TDMA-NOMA Scheme. *IEEE Access*, vol.13, 2025, pp.23384–23398. DOI: 10.1109/ACCESS.2025.3537988.
- [18] B.G., P., Naik, P.K., Patil, M. TERM: Throughput Efficient Resource Management Scheme for 5G Communication Using NOMA Systems. *International Journal of Intelligent Engineering and Systems*, vol.18, no.5, 2025, pp.609–620. DOI: 10.22266/ijies2025.0630.43.
- [19] Ju, S., Kanhere, O., Xing, Y., Rappaport, T.S. A Millimeter-Wave Channel Simulator NYUSIM with Spatial Consistency and Human Blockage. *Proc. IEEE Global Communications Conference (GLOBECOM)*, Hawaii, USA, Dec. 2019, pp.1–6.
- [20] Gadde, N., Shivaswamy, R., Siddamal, R.B.H., Gowrishankar, G., Raju, G.T., Vijay, S.S.P. Hybrid resource optimization strategy in heterogeneous wireless networks. *Indonesian Journal of Electrical Engineering and Computer Science*, vol.37, no.2, 2025, pp.829–838. DOI: 10.11591/ijeecs.v37.i2.pp829-838.

Information about the authors:

Vishalakshi – Presently carrying research work in Electronics and Communication Engineering Department, P. D. A. College of Engineering, Kalaburagi, Karnataka (An autonomous institute affiliated to Visvesvaraya Technological University (VTU), Belagavi, Karnataka) and currently working as Assistant Professor in the Department of Electronics and Communication Engineering, Faculty of Engineering and Technology, Sharnbasva University, Kalaburagi..

G. S. Biradar – Presently, he is working as a professor and HOD in Electronics and Communication dept., of P.D.A. College of Engineering, Kalaburagi, Karnataka (An autonomous institute affiliated to Visvesvaraya Technological University (VTU), Belagavi, Karnataka).

Manuscript received on 18 September 2025